# MedChemComm

Accepted Manuscript






ROYAL SOCIETY OF CHEMISTRY

www.rsc.org/medchemcomm

# Nature of the Charged Head Group Dictates the Anticancer Potential of Lithocholic Acid-Tamoxifen Conjugates For Breast Cancer Therapy

Kavita Yadav,[a,b,†] Priyanshu Bhargava,[a,†] Sandhya Bansal, [a,†] Manish Singh,[a] Siddhi Gupta,[c] Geeta Sandhu,[a] Sandeep Kumar,[a] Vedagopuram Sreekanth,[a] and Avinash Bajaj [a],*

[a]Laboratory of Nanotechnology and Chemical Biology, Regional Centre for Biotechnology, 180 Udyog Vihar, Phase I, Gurgaon-122016, Haryana, India. [b]Manipal University, Manipal, India. [c]Department of Chemistry, Indian Institute of Science Education and Research, Bhopal, India.

†These Authors contributed equally.

*Corresponding Author:

Email: bajaj@rcb.res.in, Ph: +91-124-2848831, Fax: +91-124-4038117

**Abstract:** Modulation of existing drugs is required to achieve enhanced activity for cancer therapy by lowering their effective dose. Strategies of introduction of cationic charge and hydrophobicity have been proposed and explored to enhance therapeutic effects of anticancer drugs. In this manuscript, we designed modulation of tamoxifen and synthesized eight tamoxifen (Tam) conjugated lithocholic acid (LCA) amphiphiles with variable cationic charged head groups. We unraveled anticancer potential of these amphiphiles against different breast cancer cell lines. Activity of these amphiphiles is contingent on nature of the charged head group, as hard-charged amphiphiles perform strong membrane interactions and enhanced anticancer activity as compared to soft-charged amphiphiles. In-depth mechanistic studies concluded that conjugation of dimethyl amino pyridine (DMAP) charged head group in case of LCA-Tam-DMAP enhances therapeutic effect of Tam in breast cancer cells, and makes it highly effective even against ER negative cells. Amphiphilic character of these lipid-drug conjugates can further be explored for engineering of nanotherapeutics for targeting tumors. Therefore, fine-tuning the interactions of drugs with cell membranes can help in engineering of future lipid-drug conjugates for effective cancer therapy.

**Introduction:** Cancer involving uncontrolled growth and progression of cells is going to be one of the deadly diseases across the globe. Cancer chemotherapy faces major challenges due to multiple signaling mechanisms controlling cell proliferation, angiogenesis, metastasis, efflux of anticancer drugs, development of drug resistance, delivery of existing drugs at target site, and their high systemic toxicity.[1] Therefore, modification of exiting drugs and evolution of drug delivery systems are being currently undertaken for targeting multiple pathways, lowering systemic toxicity, minimizing drug resistance, and lowering therapeutic doses.[2,3]

Tamoxifen (Tam), a lipid-soluble non-steroidal drug, is currently used for treatment of both early and advanced estrogen receptor (ER) positive breast cancer in pre- and post-menopausal women.[4] It competes with estrogen for ER, inhibits proliferation, and induces apoptosis of breast cancer cells. Systemic absorption of Tam increases risk of endometrial cancer, deep vein thrombosis, and pulmonary embolism.[4] Therefore, engineered nanomaterials, like Tam-PEGylated gold nanoparticles, have been explored for effective drug delivery for breast cancer treatment.[5] Nicolosi *et al* engineered a Tam nanoemulsion to increase its efficacy in breast cancer cell lines.[6] Jain and co-workers developed PLGA based nanoparticles for oral administration of Tam.[7] Bhattacharya and Rao have shown the use of graphene as nanocarriers for Tam and induction of apoptosis in transformed cancer cell lines of different origins.[8]

Tamoxifen, due to its lipophilic character, perform hydrophobic interactions with lipid membranes and direct interactions with intracellular receptor.[9] Tam enriches in lipid bilayer, and perturbs physical and chemical composition of biological membranes.[10] Madeira *et al* reported induction of physical changes in model and native membranes by Tam, and showed that Tam fluidizes membranes in gel phase.[11] Therefore, Tam is used for treatment of breast cancer at early stages of cancer towards ER positive and ER negative tumors.[12]

Many approaches have been developed to improve efficacy of anticancer drugs by conjugation with polymers, nanoparticles, proteins, antibodies, and dendrimers.[13] Similarly, lipid drug conjugates have been extensively explored for better interaction and permeation of drugs across cell membranes.[14] Lipidated charged head groups conjugated with anticancer drugs based on molecular hybridization techniques have recently been explored as effective anticancer therapeutics with high affinity as charged lipids are known to induce pro-apoptosis markers and reactive oxygen species. Rajkumar and co-workers have shown high therapeutic efficacy of many bioactive molecules on conjugation with cationic lipids.[15]

Bile acids present interesting scaffolds for drug delivery, due to presence of variable number of free hydroxyl groups and free acid group that can be explored for conjugation of drugs, fluorophores, and targeting ligands.[16] Marin *et al* uncovered anticancer potential of cholic acid-cisplatin conjugates in human cancer cell lines.[17] We have recently reported that bile acid-tamoxifen conjugates bearing amine head groups show irreversible interactions with membranes as compared to acid head groups.[18] Our results unraveled that amine derived cholic acid-tamoxifen conjugates bearing three tamoxifen molecules is more potent as compared to amine derived lithocholic acid-tamoxifen conjugate possessing single tamoxifen molecule. We discovered that ineffective anticancer activity of lithocholic acid-tamoxifen amphiphile is due to weak electrostatic interactions with cell membranes causing minimum membrane perturbations.[18]

In this manuscript, we hypothesize that therapeutic efficacy of lipid-drug conjugates can be modulated by introduction of variable charged head groups,[19] where hydrophobicity of lipid molecule will help in translocation of lipid-drug conjugate across membrane and different charged head groups might work as another pharmacophore by enhancing activity of anticancer drug (Figure 1a). Therefore, we synthesized eight cationic lithocholic acid-tamoxifen amphiphiles, and varied charged head group from soft-charged amine to hard-charged polar trimethyl ammonium, morpholine, 1,4-

diazabicyclo[2.2.2]octane, dimethylamino pyridine, and hard-charged non-polar pyrolidine, piperidine, and pyridine groups (Figure 1b). We studied anticancer potential of these amphiphiles against four breast cancer cell lines, and compared membrane interactions of these amphiphiles using laurdan-based hydration, DPH based anisotropy, and differential scanning calorimetry studies. Mechanistic studies, like cell cycle analysis, changes in mitochondrial potential, ROS generation assay, and western blot studies were then performed to understand the mechanism of action of potent amphiphile in ER positive (MCF-7) and ER negative (MDA-MB-231) cell lines.

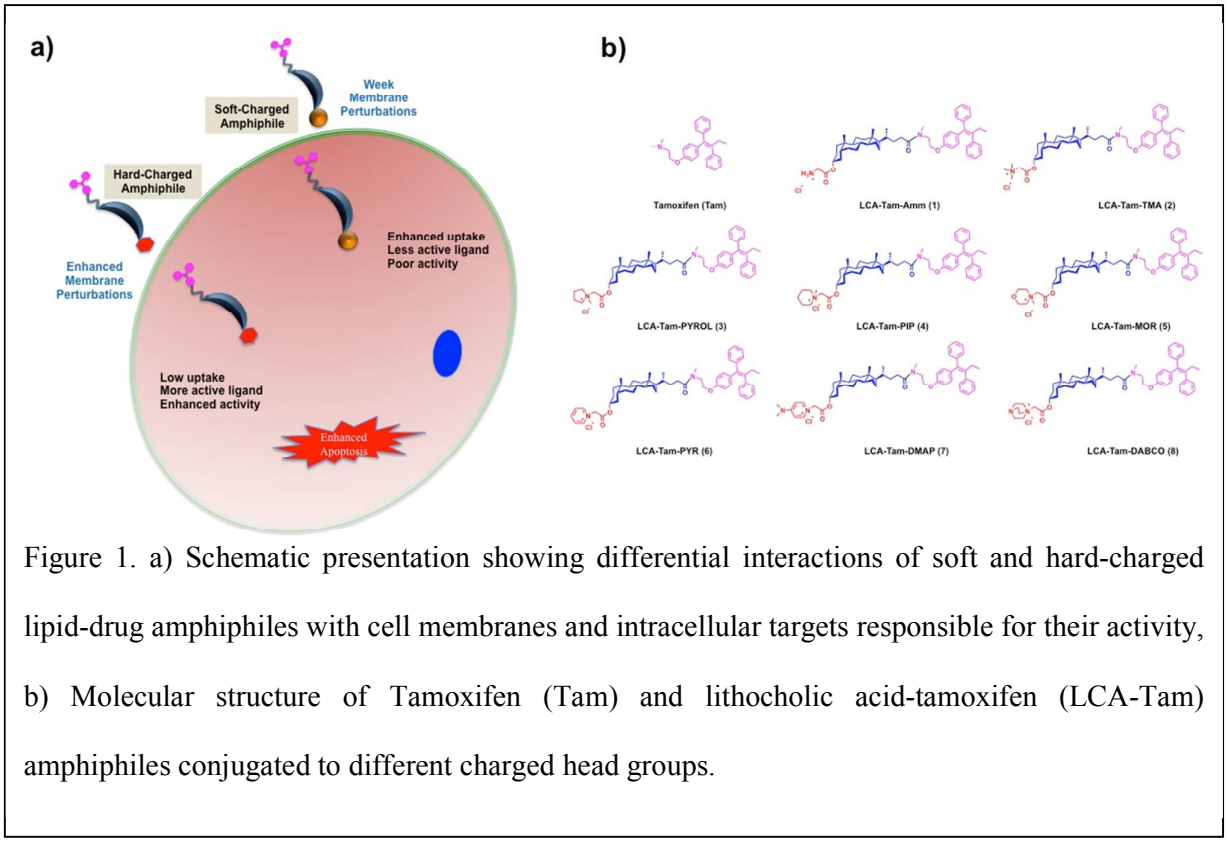


Figure 1. a) Schematic presentation showing differential interactions of soft and hard-charged lipid-drug amphiphiles with cell membranes and intracellular targets responsible for their activity, b) Molecular structure of Tamoxifen (Tam) and lithocholic acid-tamoxifen (LCA-Tam) amphiphiles conjugated to different charged head groups.

**Results and Discussion:**

**Synthesis of LCA-Tam amphiphiles:** Lithocholic acid was conjugated to desmethylated tamoxifen[18] by DCC/DMAP coupling (Scheme 1) that was further reacted with chloroacetylchloride for 12h at 60 °C. Chloroacetyl chloride derivative of lithocholic acid-tamoxifen conjugate was then quaternized with different amine head groups to get final lipid-drug conjugates. All lipid-drug conjugated amphiphiles were characterized by $^{1}$H-NMR, $^{13}$C-NMR, HRMS, and HPLC (ESI).

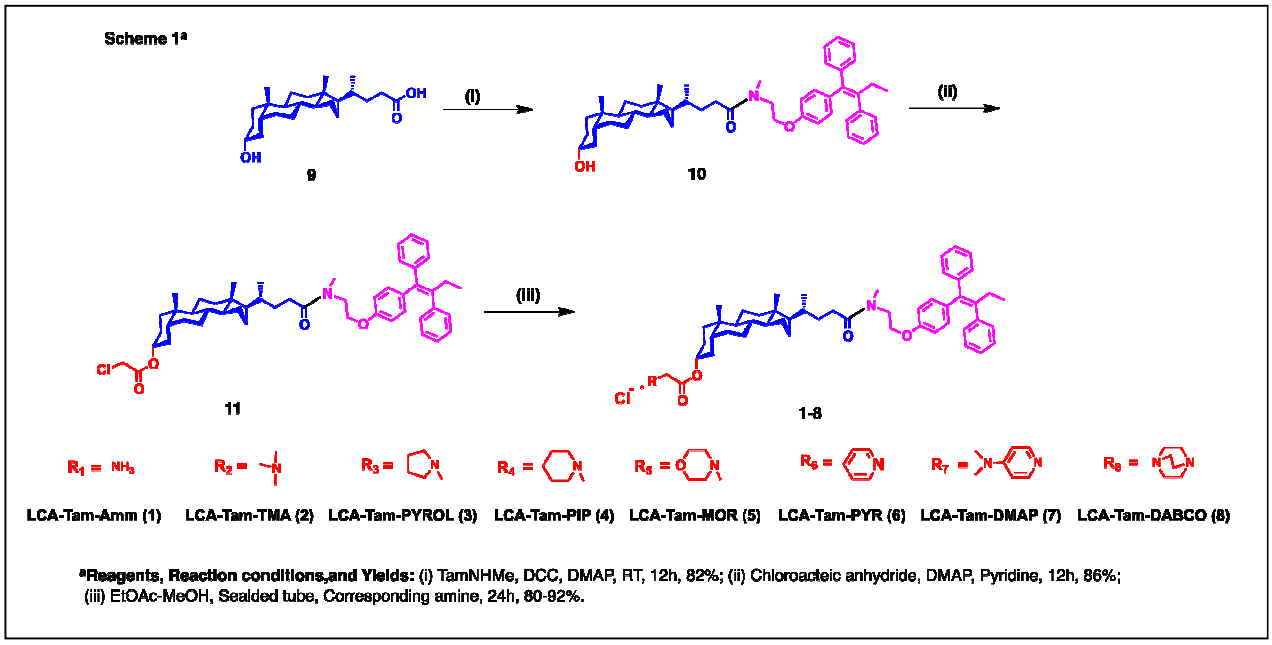


**Anticancer Activities of LCA-Tam Amphiphiles:** We studied anticancer potential of Tam, and lithocholic acid-tamoxifen (LCA-Tam) amphiphiles in four human breast cancer cell lines, MDA-MB-468 (ER negative), T47D (ER positive), MCF-7 (ER positive), and MDA-MB-231 (ER negative) at 1, 5, 10, 20 and 50 μM concentrations after 48h of treatment (Fig. S1, ESI). We observed that cytotoxicity of amphiphiles is contingent on nature of charged head group and cell line. Structure activity studies as shown in Table 1 suggested that a) conjugation of soft-charged ammonium head group (LCA-Tam-Amm) does not enhance

anticancer potential of Tam in any of the cell lines; b) hard-charged amphiphiles are in general more effective than soft-charged amphiphile (LCA-Tam-Amm) for its anticancer activity; c) hydrophobic head group derived amphiphiles like LCA-Tam-PIP, LCA-Tam-PYROL and LCA-Tam-DMAP are most effective across different cell lines; d) polar hydrophobic head group derived amphiphile LCA-Tam-Amm, LCA-Tam-TMA, LCA-Tam-MOR are least effective in different cell lines; e) surprisingly, hard-charged amphiphiles are highly effective in ER negative MDA-MB-231 and MDA-MB-468 cells (Table 1). As observed presviously, conjugation of primary amine (soft-charge) derived amphiphile make Tamoxifen ineffective against breast cancer cell lines.[18]

LCA-Tam-DMAP was most potent having $IC_{50}$ values of 6.5, 12.72, 3.13 and 7.0 μM in MDA-MB-231, MCF-7, MDA-MB-468 and T47D cell lines respectively (Table 1). Variations in toxicity of LCA-Tam-DMAP among ER +ve or ER –ve cell lines themselves might be due to different genomic and proteomic nature of cell lines. LCA-Tam-DMAP was ~4-5 fold more effective as compared to Tam in ER negative MDA-MB-231 and MDA-MB-468 cells whereas it is 4-fold more active in ER positive T47D cells and did not enhance activity in MCF-7 cells. Conjugation of DMAP to LCA-Tam conjugate makes it highly effective against ER -ve cells as well. We then compared cytotoxicity of LCA-Tam-DMAP amphiphiles with LCA-DMAP amphiphile possessing no tamoxifen molecule attached (Table 1; Fig. S2, ESI). Comparative cytotoxicity profiles of LCA-DMAP and LCA-Tam-DMAP clearly suggest that conjugation of Tamoxifen to LCA-DMAP amphiphile enhances the anticancer potential by ~2.0-3.5 fold in MDA-MB-231, MCF-7, MDA-MB-468, and T47D cells.

**Table 1.** Anticancer activities ($IC_{50}$) of lithocholic acid-tamoxifen (LCA-Tam) amphiphiles against breast cancer cell lines.[a]

| Amphiphile | MDA-MB-231 (ER -ve) | MCF-7 (ER +ve) | MDA-MB-468 (ER –ve) | T47D (ER +ve) | RT (min)[b] |
|---|---|---|---|---|---|
| **Tam** | 27.0 ± 2.7 | 12.5 ± 0.30 | 14.99 ± 1.20 | 29.9 ± 0.5 | -[c] |
| **LCA-Tam-Amm** | > 50 | > 50 | > 50 | >50 | -[c] |
| **LCA-Tam-TMA** | 18.11 ± 0.43 | 28.87 ± 5.28 | 14.95 ± 0.67 | 8.1 ± 0.4 | 6.676 |
| **LCA-Tam-PYROL** | 12.64 ± 0.35 | 24.0 ± 3.69 | 6.61 ± 0.43 | 8.4 ± 0.15 | 6.790 |
| **LCA-Tam-PIP** | 9.2 ± 0.38 | 24.53 ± 1.39 | 7.6 ± 0.42 | 9.8 ± 0.15 | 6.767 |
| **LCA-Tam-MOR** | 48.2 ± 1.37 | 43.62 ± 3.33 | 15.33 ± 2.72 | 45.2 ± 0.76 | 6.741 |
| **LCA-Tam-PYR** | 18 ± 1.32 | >50 | 13.55 ± 0.42 | 17.4 ± 0.12 | 7.033 |
| **LCA-Tam-DMAP** | 6.5 ± 0.1 | 12.72 ± 0.27 | 3.13 ± 0.72 | 7.0 ± 0.08 | 6.837 |
| **LCA-Tam-DABCO** | 20.0 ± 2.40 | >50 | 20.85 ± 2.56 | 17.9 ± 0.08 | 6.735 |
| **LCA-DMAP** | 13.72 ± 0.16 | 43.4 ± 2.65 | 9.10 ± 0.64 | 13.3 ± 0.29 | -[c] |

a: All values are $IC_{50}$ values in μM with SD; b: retention time in HPLC ($CH_3CN$:MeOH:70:30); c: not determined.

**Interactions of LCA-Tam amphiphiles:** To unravel the influence of soft and hard-charged amphiphiles on membrane interactions, we studied interactions of Tam, least effective LCA-Tam-Amm amphiphile, and most effective LCA-Tam-DMAP amphiphile with model membranes using Laurdan based hydration, DPH based anisotropy, and differential scanning calorimetry (DSC) studies and compared with LCA-DMAP. Laurdan fits in membrane lipids with its dimethylamino pyridine group at surface, and is sensitive to change in surface hydration.[20] Laurdan-doped membrane vesicles were incubated with amphiphiles, and changes in generalized polarization (GP) of Laurdan were measured at regular intervals. Laurdan studies suggested that GP decreases on incubation of liposomes with LCA-DMAP and LCA-Tam-DMAP whereas no change in GP was observed on incubation with LCA-Tam-Amm (Figure 2a). Presence of hard charge in case of LCA-Tam-DMAP induces strong membrane interactions and maximum dehydration of membranes, whereas LCA-Tam-Amm

and Tam shows weak interactions with membranes without significant change in hydration of membranes (Figure 2a).

We then determined changes in membrane fluidity of liposomes by measuring fluorescence anisotropy of DPH fluorophore in liposomal membranes on incubation with amphiphiles.[21] We observed a time dependent decrease in fluorescence anisotropy of DPH in membranes that is contingent on nature of amphiphiles (Figure 2b) suggesting the increase in fluidity of membranes. Tam and LCA-Tam-Amm lowers fluorescence anisotropy in the same order suggesting that LCA-Tam-Amm induces Tam-mediated interactions with membranes (Figure 2b), whereas LCA-Tam-DMAP lowers anisotropy to a greater extent suggesting enhanced induction of membrane fluidity as compared to Tam and LCA-Tam-Amm. Therefore, conjugation of Tam to hard-charged cationic amphiphiles induces more fluidic effect on membranes and therefore might induce more cytotoxicity as compared to Tam.

To understand thermodynamics of these interactions, we studied effect of Tam, LCA-DMAP, and LCA-Tam-DMAP on model membranes by DSC.[22] Tam induces minor change in broadness of main transition peak indicating poor interactions with DPPC membranes (Figure 2c). LCA-DMAP and LCA-Tam-DMAP induces broadness in DPPC vesicles along with lowering of phase transition temperature ($T_m$) suggesting strong interactions with DPPC membranes. Therefore, above studied suggested that hard-charged LCA-Tam-DMAP induces strong membrane perturbations as compared to soft-charged LCA-Tam-Amm amphiphile.

Enhanced toxicity of LCA-Tam-DMAP might be either due to a) enhanced membrane perturbations; b) enhanced penetration of LCA-Tam-DMAP in cancer cells, or c) combined intracellular toxicity of LCA-DMAP and Tam. Membrane hydration and membrane fluidity studies showed that LCA-Tam-DMAP induces enhanced membrane perturbations. Therefore, to further explore the uptake of LCA-Tam-DMAP, we compared the cellular uptake of fluorophore conjugates of Tam and LCA-DMAP in MDA-MB-231 and MCF-7 cells. We

synthesized LCA-DMAP-NBD and Tam-NBD conjugates where fluorophore (NBD) is conjugated to LCA-DMAP and Tamoxifen (ESI). FACS studies of Tam-NBD and LCA-DMAP-NBD in MCF-7 and MDA-MB-231 cells suggested the more accumulation of Tam-NBD inside the cells as compared to LCA-DMAP-NBD (Fig. S3, ESI). Therefore, conjugation of DMAP in case of LCA-DMAP-NBD does not help in its high accumulation inside the cells in spite of enhanced membrane perturbations. Therefore, high therapeutic efficacy of LCA-Tam-DMAP might be due to enhanced membrane perturbations and combined effect of Tamoxifen and DMAP pharmacophore and their intracellular action. We then investigated the mechanism of LCA-Tam-DMAP against ER negative MDA-MB-231 cells and ER positive MCF-7 cells.

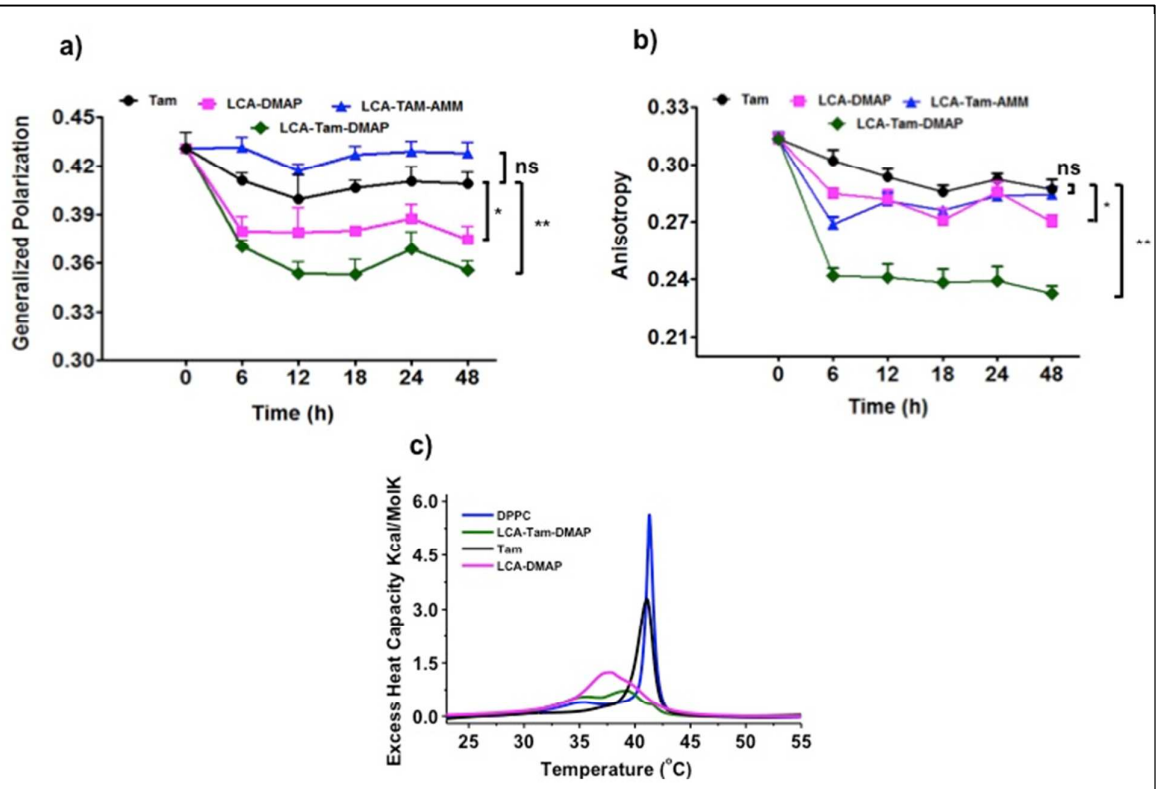


Figure 2. a) Changes in generalized polarization of Laurdan in model membranes on interactions with Tam, LCA-DMAP, LCA-Tam-Amm and LCA-Tam-DMAP (* $p < 0.023$; ** $p < 0.007$); b) Changes in fluorescence anisotropy of DPH in model membranes on interactions with Tam, LCA-DMAP, LCA-Tam-Amm and LCA-Tam-DMAP (* $p < 0.029$; ** $p < 0.003$); c) Differential scanning thermograms of model membranes on interactions with Tam, LCA-DMAP and LCA-Tam-DMAP.

**Cell Cycle Studies:** We analyzed the fate of cells in different phases of cell cycle on treatment with Tam, LCA-DMAP, and LCA-Tam-DMAP in MDA-MB-231 and MCF-7 cells. There is a concentration dependent increase in number of cells in sub $G_0$ phase of cell cycle suggesting the arrest of cells before entering cell cycle. We observed a three-fold increase in

number of cells in sub $G_0$ after treatment with 20 μM of Tam, whereas a five-fold increase in sub $G_0$ was observed on treatment with 20 μM of LCA-Tam-DMAP in MDA-MB-231 cells (Figure 3a). Similarly, we observed six-fold increase in sub $G_0$ phase after treatment with LCA-Tam-DMAP in MCF-7 cells, whereas Tam induced two-fold enhancement in sub $G_0$ cells (Figure 3b). LCA-DMAP without Tam conjugation could induce only minor changes cell cycle of both the cell lines. Therefore, these studies concluded that conjugation of Tam to LCA-DMAP amphiphile enhances the anticancer potential of Tam in MDA-MB-231 and MCF-7 cells.

**Change in mitochondrial transmembrane potential ($\Delta\psi_m$):** Change in mitochondrial membrane potential is important consequence of apoptosis leading to release of cytochrome c from mitochondria followed by activation of caspases.[23] We investigated the effect of Tam, LCA-DMAP, and LCA-Tam-DMAP on change in mitochondrial membrane potential in MDA-MB-231 and MCF-7 cells using 3,3′-dihexyloxacarbocyanine iodide [$DiOC_6$]. We observed that LCA-Tam-DMAP induces maximum change of membrane potential in MDA-MB-231 cells, suggesting the disruption of membrane integrity (Figure 4), whereas Tam did not induce any change in mitochondrial membrane potential in MDA-MB-231 cells. Surprisingly, we have not observed any change in mitochondrial potential of MCF-7 cells using [$DiOC_6$] on treatment with Tam and LCA-Tam-DMAP. Incubation of LCA-DMAP alone also induces disruption of mitochondrial membranes only in MDA-MB-231 cells. Therefore, these results suggest that conjugation of DMAP charged head group induces selective mitochondrial membrane disruptions in ER negative MDA-MB-231 cells, and therefore is responsible for enhanced selective activity against MDA-MB-231 cells.

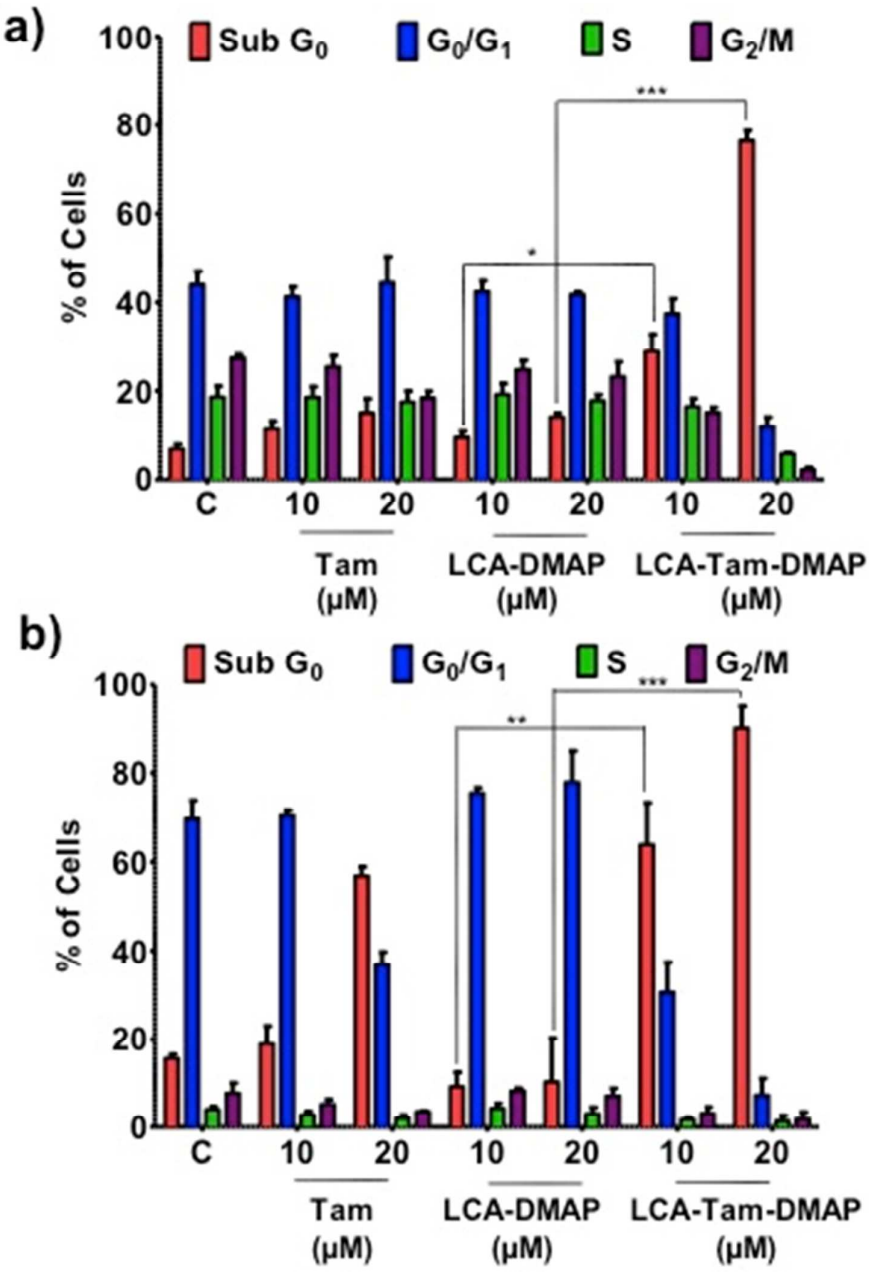


Figure 3. Cell cycle analysis in (a) MDA-MB-231 and (b) MCF-7 breast cancer cell lines treated with Tam, LCA-DMAP, and LCA-Tam-DMAP at 10 and 20 μM concentrations after 48 h. (* $p < 0.05$; ** $p < 0.005$; *** $p < 0.0005$)

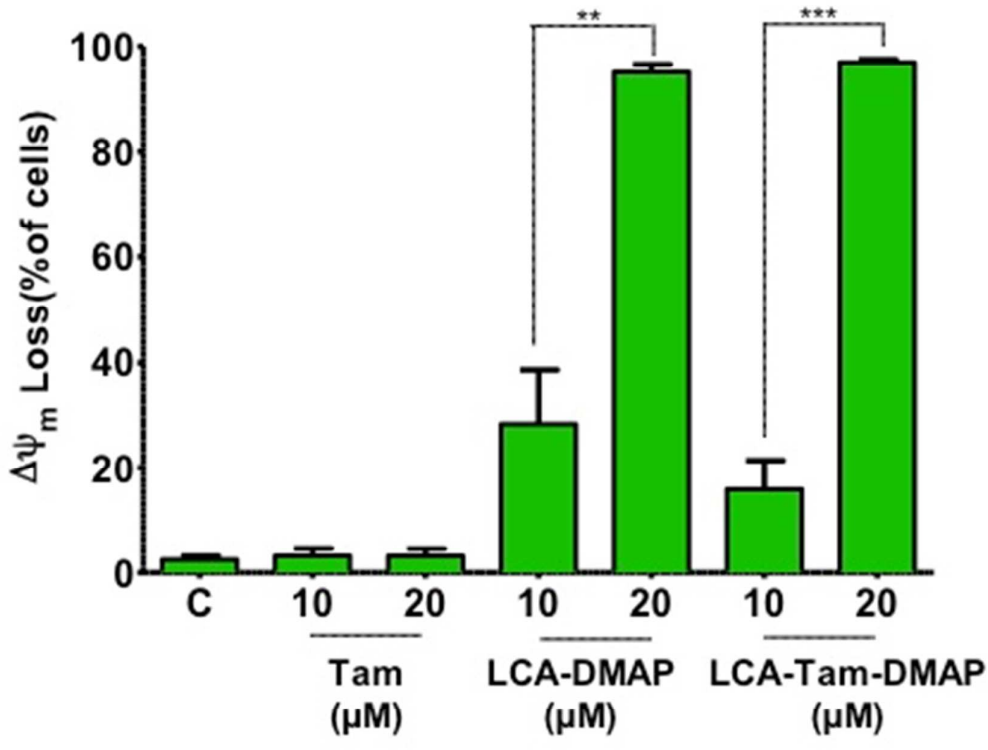


Figure 4, Membrane potential measurements in MDA-MB-231 cells using $DiOC_6$ dye after treatment with Tam, LCA-DMAP, and LCA-Tam-DMAP at 10 and 20μM for 48h. (** $p < 0.005$; *** $p < 0.0005$)

**Generation of Reactive Oxygen Species:** We then measured the intracellular ROS levels in MDA-MB-231 and MCF-7 cells on treatment with Tam, LCA-DMAP, and LCA-Tam-DMAP. There was ~1.8 fold increase in ROS levels on treatment with 20 μM of Tam after 60 min in MDA-MB-231 cells, whereas ~2.3 fold increase in ROS levels is observed after treatment with LCA-Tam-DMAP (Figure 5a). We have not observed enhanced ROS levels in MCF-7 cells on treatment with LCA-Tam-DMAP (Figure 5b). Therefore, these results suggested that LCA-Tam-DMAP is highly selective in inducing enhanced ROS levels, and increased disruptions in mitochondrial membrane potential in ER negative MDA-MB-231 cells as compared to ER positive MCF-7 cells. This enhanced ROS levels and disruptions in mitochondrial membranes induced arrest of cells in sub-$G_0$ phase, further leading to apoptosis.

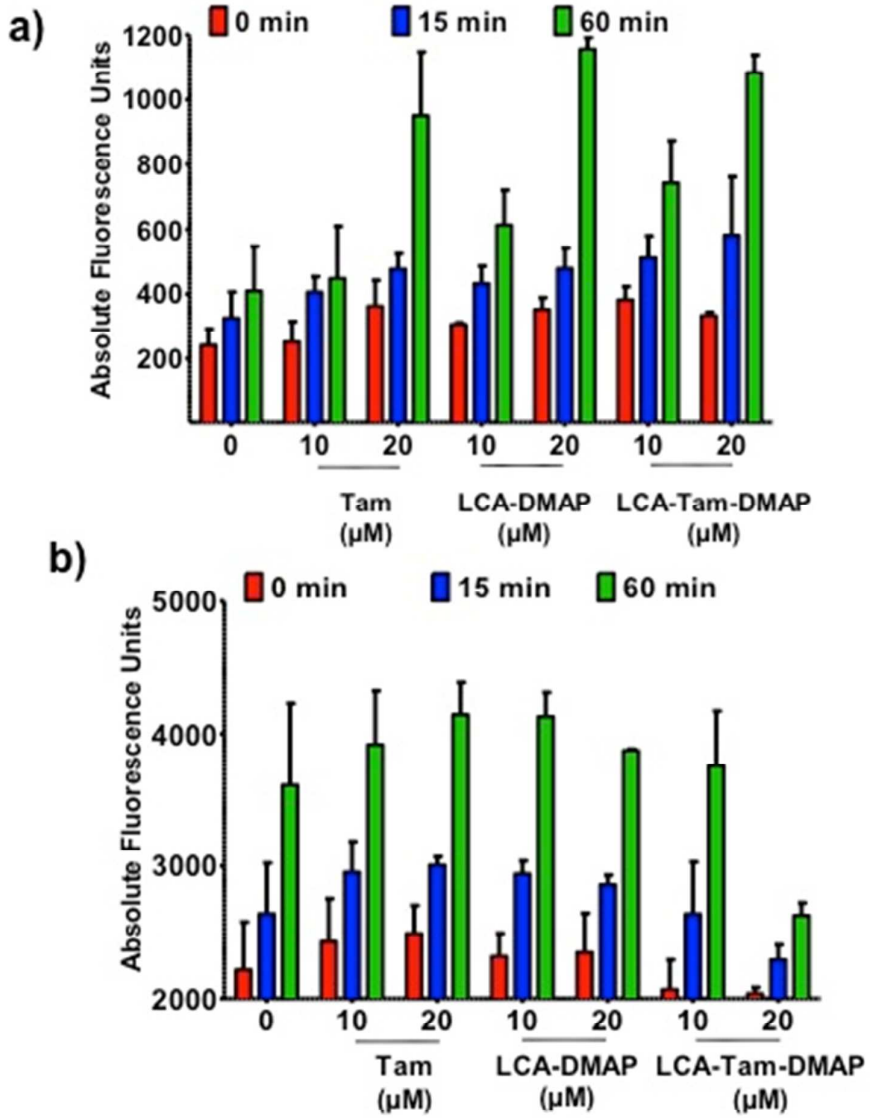


Figure 5. ROS measurements in (a) MDA-MB-231 and (b) MCF-7 cells after treatment with Tam, LCA-DMAP, and LCA-Tam-DMAP at 10 and 20 μM after 15 and 60 min.

**Regulation of anti-apoptotic and pro-apoptotic proteins:** We then studied the influence of Tam, LCA-DMAP and LCA-Tam-DMAP on expression of pro-apoptotic, anti-apoptotic, and caspase proteins in MDA-MB-231 and MCF-7 cells. Our western blot studies suggested that pro-apoptotic Bax is up regulated in MDA-MB-231 cells after treatment with LCA-Tam-DMAP (Figure 6a). Anti-apoptotic protein Bcl-2 levels gets down regulated with no change in Bcl-xL protein expression on treatment with LCA-Tam-DMAP in MDA-MB-231 cells. We observed increased levels of cleaved caspase 6, 7 and 8, whereas no change was observed in levels of caspase 9. As mitochondria is both source and target of ROS,[24] mitochondria and ROS are key players of apoptosis in MDA-MB-231 cells. Release of cytochrome c from mitochondria triggering caspase activation appears to be largely mediated by direct or indirect action of ROS. Cell membranes show enhanced membrane interactions for LCA-Tam-DMAP resulting in enhanced ROS levels. Therefore, disruption of mitochondrial membrane and more cytochrome c release induces caspase activation, and enhances apoptotic effect of LCA-Tam-DMAP.

In MCF-7 cells, we observed down regulation of Bcl-2 and Bcl-xL, whereas Bax levels remain unchanged after treatment with LCA-Tam-DMAP. It is known that caspase 8 initiates apoptosis in response to ligand binding to cell surface receptors and caspase 9 activates apoptosis through release of cytochrome c from the mitochondrial matrix. Caspase 3 amplifies signals from caspase 8 and caspase 9. We have not observed no caspase 3 in MCF-7 cell as established in earlier reports.[25] Therefore, absence of caspase 3 leads to decrease in apoptotic signals *via* caspase 8 and 9. Therefore we did not observe any activation of caspase 9 in MCF-7 cell lysates. However, we observed overall decrease in pro and active caspase 8 suggesting that apoptosis in not induced by extrinsic pathway in MCF-7 cells. Similarly we observed decrease in levels of caspase 6 and 7 which are executioner caspases on treatment

with LCA-Tam-DMAP. Therefore, LCA-Tam-DMAP induces apoptosis in MCF-7 where caspases play intermediary roles.

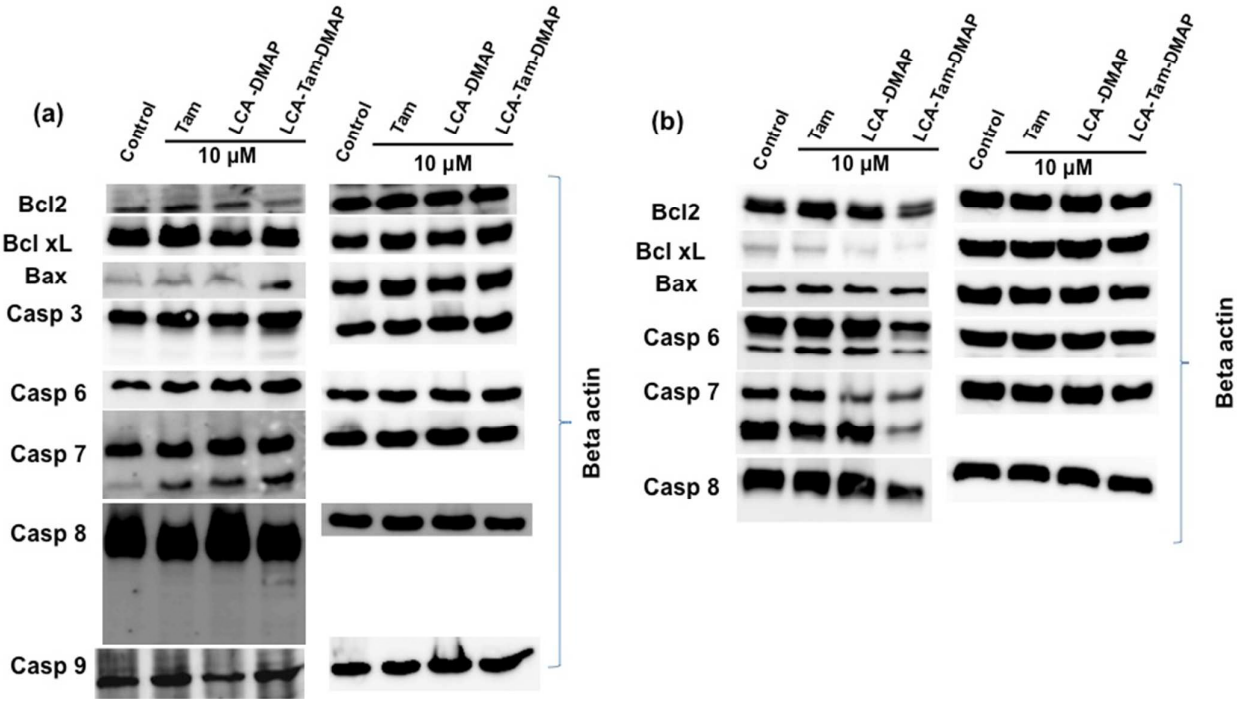


Figure 6. Western blots of (a) MDA-MB-231 and (b) MCF7 cell lines on treatment with Tam, LCA-DMAP, and LCA-Tam-DMAP at 10µM for 48h showing regulation of pro-apoptotic, anti-apoptotic, and caspase proteins.

## Conclusions

We have designed and studied the anticancer potential of eight cationic lipid-drug conjugates, where tamoxifen was conjugated to carboxyl group of lithocholic acid, and hydroxyl group of lithocholic acid was quaternized with different cationic charged head groups. SAR studies unraveled that anticancer activity of amphiphiles against four breast cancer cells is strongly contingent on nature of the charged head group. Membrane binding studies concluded that strong electrostatic interactions followed by favourable membrane intercalation are critical for enhanced activity of LCA-Tam-DMAP, whereas soft-charged LCA-Tam-Amm perform weak interactions with membranes accounting for its inactive action. LCA-Tam-DMAP amphiphile is highly potent against ER negative MDA-MB-231 cells due to increased levels of ROS generation and targeting mitochondrial membrane permeability. Mechanistic studies showed down-regulation of anti-apoptotic and up-regulation of pro-apoptotic proteins responsible for apoptosis. This study suggest that conjugation of different charged head groups can be explored further for engineering of new lipid-drug amphiphiles that would have enhanced therapeutic effect for future cancer therapy. Due to amphiphilic nature of these lipid-drug conjugates, in future, we would be engineering the nanoparticles from these conjugates for tumor targeting. These nanoparticles would be explored for *in vivo* anticancer activities in xenograft models, as nanoparticles would have tendency for tumor targeting due to enhanced permeation and retention effect.

## Experimental Section

**Materials and methods:** All the solvents and chemicals used are of ACS grade. Lithocholic acid, tamoxifen, chloroacetic anhydride, diphenylhexatriene (DPH), and laurdan were purchased from Sigma-Aldrich. DPPC was purchased from Avanti Polar Lipids, USA. All the compounds were purified using Combi-flash chromatography using silica gel redi-sep columns. $^{1}$H-NMR and $^{13}$C-NMR spectra were recorded on Brucker-Avance-400 MHz FT-

NMR spectrometer. Chemical shifts are reported in δ ppm reference to $CDCl_3$ for $^1$H-NMR. All the mass spectra were recorded with AB SCIEX Triple TOF 5600 system.

**Synthesis of lithocholic acid-tamoxifen amphiphiles:**

**Synthesis of lithoholic acid-tamoxifen conjugate (LCA-Tam, 10):** Lithocholic acid (2 gm, 0.005 mol) was taken in dry DCM in 250 mL round bottomed flask, followed by addition of desmethyl tamoxifen[18] (1.78 gm, 0.005 mol), DCC (1.08 gm, 0.00525 mol), DMAP (0.183 gm, 0.0015 mol). Reaction was performed at room temperature for 12h under anhydrous conditions. After 12h, reaction mixture was washed with water, brine; and dried over anhydrous $Na_2SO_4$. Pure product was obtained by column chromatography under EtOAc:Pet Ether 55:45. Yield: 3.12 gm. (82.0 %). $^1$H-NMR ($CDCl_3$, 400 MHz) δ: 0.63 (s, 3H, -C*H*$_3$), 0.88-2.04 (m, 37H), 2.43-2.46 (m, 2H, -CH$_2$-C*H*$_2$-CO-N), 3.07 (s, 3H, -N-C*H*$_3$), 3.59-3.65 (m, 3H, -N-CH$_2$-C*H*$_2$-O-, -O-C*H*), 4.0 (t, 2H, J = 5.2 Hz, -N-C*H*$_2$-CH$_2$-O-), 6.53 (m, 2H, Ar*H*), 6.79 (d, 2H, J = 8.0Hz, Ar*H*), 7.10-7.35 (m, 10H, Ar*H*). $^{13}$C-NMR ($CDCl_3$, 400 MHz) δ: 173.9, 156.5, 143.7, 143.6, 142.4, 141.6, 141.4, 138.2, 135.6, 131.9, 129.6, 129.4, 128.1, 127.9, 127.8, 126.5, 126.0, 113.2, 71.7, 66.5, 56.5, 56.0, 49.1, 47.9, 42.7, 42.1, 40.4, 40.2, 37.5, 36.4, 35.8, 35.5, 34.5, 33.9, 31.4, 30.9, 30.5, 30.4, 29.9, 29.7, 29.0, 28.2, 27.2, 26.4, 25.6, 25.1, 24.9, 24.2, 23.3, 20.8, 18.5, 13.5, 12.0. MS (ESI) m/z calcd for $C_{49}H_{65}NO_3$ (716.04), found (715.86) $[M]^+$.

**Synthesis of chloroacetyl derivative of LCA-Tam (11):** Lithocholic acid-Tam (2.5 gm. 0.0035 mol) was taken in a 250 mL round bottomed flask in dry toluene followed by addition of chloroacetic anhydride (0.84 gm. 0.0049 mol), DMAP (0.128 gm. 0.001 mol), and pyridine (2 mL) under anhydrous condition. Reaction mixture was refluxed for 12h, and then toluene was evaporated off under vacuum, and reaction mixture was washed with brine water and dried over $Na_2SO_4$. Pure product was obtained by column chromatography using EtOAc:Hexane (12:82) as solvent system. Yield 2.4 g (86.3 %). $^1$H NMR ($CDCl_3$, 400 MHz)

δ: 0.63 (s, 3H, -C*H*$_3$), 0.79-2.17 (m, 37H), 2.42-2.47 (m, 2H, -CH$_2$-C*H*$_2$-CO-N), 3.07 (s, 3H, -N-C*H*$_3$), 3.63-3.65 (m, 2H, -N-CH$_2$-C*H*$_2$-O-), 3.73 (t, 2H, J = 5.5 Hz, -N-C*H*$_2$-CH$_2$-O- ), 3.98 (s, 2H, CO-C*H*$_2$-Cl), 4.79-4.85 (m, 1H, -O-C*H*), 6.53 (d, 2H, J = 9.0Hz, Ar*H*), 6.79 (d, 2H, J = 9.0Hz, Ar*H*), 7.02-7.47 (m, 10H, Ar*H*). $^{13}$C-NMR (CDCl$_3$, 400 MHz) δ: 173.9, 166.8, 156.5, 143.7, 142.4, 141.6, 138.2, 136.1, 135.6, 131.9, 129.6, 129.4, 128.1, 127.9, 126.5, 126.0, 113.2, 66.5, 65.1, 56.4, 56.1, 49.1, 47.9, 42.7, 41.9, 41.2, 40.4, 40.1, 37.5, 35.8, 35.5, 34.9, 32.0, 31.3, 30.9, 30.4, 29.7, 29.0, 28.2, 27.0, 26.4, 25.6, 24.9, 24.2, 23.2, 20.8, 18.5, 13.5, 12.0. MS (ESI) m/z calcd for $C_{51}H_{66}ClNO_4$ (792.52), found (791.86) $[M]^+$.

**Synthesis of LCA-Tam amphiphiles (1-8):** Chloroacetyl derivative of LCA-Tam (**11**) was refluxed with corresponding tertiary amine in ethyl acetate in pressure tube for 24h. After completion of reaction, solvent was removed and final product was purified by repeated precipitation in ethyl acetate. All the final amphiphiles were characterized by $^1$H-NMR, $^{13}$C-NMR, HRMS, and HPLC (ESI).

**LCA-Tam-Amm:** Yield 80 % $^1$H-NMR (CDCl$_3$, 500 MHz) δ: 0.628 (s, 3H, -C*H*$_3$), 0.755-2.4 (m, 46H), 2.41-2.49 (q, 2H, J = 7.2 Hz, -C*H*$_2$CH$_3$),, 2.936-3.067 (d, 3H, -N-C*H*$_3$), 3.43-3.50 (m, 2H, -N-CH$_2$-C*H*$_2$-O-), 3.89 (t, 2H, J = 5.5 Hz, -N-C*H*$_2$-CH$_2$-O- ), 3.6 (s, 2H, CO-C*H*$_2$-N$^+$-), 4.77 (m, 1H, -O-C*H*), 6.58 (d, 2H, J = 8.5Hz, Ar*H*), 6.72 (d, 2H, J = 8.5Hz, Ar*H*), 7.07-7.46 (m, 10H, Ar*H*). $^{13}$C-NMR (CDCl$_3$, 400 MHz) δ: 174.0, 173.8, 156.5, 143.7, 142.4, 141.4, 138.1, 135.6, 131.9, 129.6, 129.4, 128.1, 127.8, 126.5, 126.0, 113.2, 71.8, 66.5, 56.5, 56.0, 47.9, 42.7, 42.1, 40.4, 40.1, 37.5, 36.5, 35.8, 35.3, 34.5, 33.8, 30.9, 30.5, 29.0, 28.2, 27.2, 26.4, 24.2, 23.3, 20.8, 18.5, 13.5, 12.0. ESI-MS: m/z calculated for $C_{55}H_{78}ClN_3O_4$: 809.55, found: 773.39 $[M]^+$.

**LCA-Tam-TMA:** Yield 92 % $^1$H-NMR (CDCl$_3$, 500 MHz) δ: 0.632 (s, 3H, -C*H*$_3$), 0.89-2.4 (m, 52H), 2.41-2.49 (q, 2H, J = 7.2 Hz, -C*H*$_2$CH$_3$), 2.9-3.06 (d, 3H, -N-C*H*$_3$), 3.60 (s, 10H, -N(C*H*$_3$)$_3$, -N-CH$_2$-C*H*$_2$-O-), 3.9 (m, 2H, -N-C*H*$_2$-CH$_2$-O- ), 4.8 (m, 3H, CO-C*H*$_2$-N$^+$-, -O-

C*H*), 6.57 (d, 2H, J = 8.0Hz, Ar*H*), 6.72 (d, 2H, J = 8.5Hz, Ar*H*), 7.09-7.46 (m, 10H, Ar*H*). $^{13}$C-NMR ($CDCl_3$, 400 MHz) δ: 164.2, 156.3, 143.7, 142.4, 132.0, 131.9, 129.6, 129.4, 128.1, 127.8, 126.5, 126.0, 113.2, 108.4, 66.5, 63.4, 60.3, 56.3, 54.3, 42.7, 41.9, 40.4, 40.0, 37.5, 37.2, 35.7, 35.4, 34.8, 34.5, 30.9, 29.0, 26.9, 26.4, 24.1, 23.2, 21.0, 20.8, 18.5, 14.2, 13.5, 12.0. ESI-MS: m/z calculated for $C_{54}H_{75}ClN_2O_4$: 851.63, found: 815.42 $[M]^+$.

**LCA-Tam-PYROL:** Yield: 79.6 %. $^1$H-NMR ($CDCl_3$, 500 MHz) δ: 0.63 (s, 3H, -C*H*$_3$), 0.896-2.4 (m, 52H), 2.41-2.49 (q, 2H, J = 7.2 Hz, -C*H*$_2$CH$_3$), , 2.9-3.1 (d, 3H, -N-C*H*$_3$), 3.52 (s, 3H, -N$^+$-C*H*$_3$), 3.65 (t, 2H, J = 5.5Hz, -N-CH$_2$-C*H*$_2$-O-), 3.82-3.91 (m, 2H, -N-C*H*$_2$-CH$_2$-O-), 4.02-4.2 (m, 4H, -N$^+$-(C*H*$_2$)$_2$), 4.78 (m, 1H, -O-C*H*), 4.90-5.1 (s, 2H, CO-C*H*$_2$-N$^+$-), 6.51 (d, 2H, J = 7.0Hz, Ar*H*), 6.78 (d, 2H, J = 8.0Hz, Ar*H*), 7.15-7.47 (m, 10H, Ar*H*). $^{13}$C-NMR ($CDCl_3$, 400 MHz) δ: 173.7, 164.8, 143.7, 142.5, 141.4, 138.2, 135.6, 131.9, 131.8, 129.6, 129.4, 128.1, 127.9, 127.8, 126.5, 126.0, 113.2, 66.5, 65.2, 62.5, 56.3, 55.9, 49.0, 47.9, 42.7, 41.9, 40.4, 40.0, 37.5, 35.7, 35.4, 34.8, 34.5, 32.0, 30.3, 29.0, 28.2, 26.4, 24.1, 23.2, 21.3, 20.8, 18.5, 13.5, 12.0. ESI-MS: m/z calculated for $C_{56}H_{77}ClN_2O_4$: 877.67, found: 841.43 $[M]^+$.

**LCA-Tam-PIP:** Yield: 71 % $^1$H-NMR ($CDCl_3$, 500 MHz) δ: 0.63 (s, 3H, -C*H*$_3$), 0.896-2.4 (m, 52H), 2.41-2.49 (q, 2H, J = 7.2 Hz, -C*H*$_2$CH$_3$), 2.42-2.45 (m, 4H, - 2 x -N$^+$-CH$_2$-C*H*$_2$), 2.9-3.06 (d, 3H, -N-C*H*$_3$), 3.53 (s, 3H, -N$^+$-C*H*$_3$), 3.65 (t, 2H, J = 5.5Hz, -N-CH$_2$-C*H*$_2$-O-), 3.88 (m, 2H, -N$^+$-C*H*$_2$), 3.95 (t, 2H, J = 5.5Hz, -N-C*H*$_2$-CH$_2$-O-), 4.10 (m, 2H, -N$^+$-C*H*$_2$), 4.74 (s, 2H, CO-C*H*$_2$-N$^+$-), 4.80 (m, 1H, -O-C*H*), 6.51 (d, 2H, J = 6.5Hz, Ar*H*), 6.78 (d, 2H, J = 8.5Hz, Ar*H*), 7.01-7.47 (m, 10H, Ar*H*). $^{13}$C-NMR ($CDCl_3$, 400 MHz) δ: 173.7, 156.5, 142.4, 138.2, 131.9, 129.6, 129.4, 128.1, 127.8, 126.5, 126.0, 113.2, 66.5, 61.6, 56.3, 47.9, 42.7, 41.9, 40.4, 40.0, 37.5, 35.7, 35.4, 34.8, 34.5, 31.9, 29.0, 28.2, 26.9, 26.4, 26.2, 24.1, 23.2, 20.8, 20.2, 18.5, 13.5, 12.0. ESI-MS: m/z calcd. for $C_{57}H_{79}ClN_2O_4$: 891.70, found: 855.44 $[M]^+$.

**LCA-Tam-MOR:** Yield: 80.8 %. $^{1}$H-NMR ($CDCl_3$, 500 MHz) δ: 0.63 (s, 3H, -C*H*$_3$), 0.82-2.24 (m, 52H), 2.41-2.49 (q, 2H, J = 7.2 Hz, -C*H*$_2$CH$_3$),, 3.93-3.06 (d, 3H, -N-C*H*$_3$), 3.7 (s, 3H, -N$^+$-C*H*$_3$), 3.65 (m, 2H, -N-CH$_2$-C*H*$_2$-O-), 3.80 (m, 2H, -N-C*H*$_2$-CH$_2$-O- ), 3.95-4.16 (m, 8H, -N$^+$-(CH$_2$)$_2$-O-(CH$_2$)$_2$), 4.78-4.83 (m, 1H, -O-C*H*), 5.27 (s, 2H, CO-C*H*$_2$-N$^+$-), 6.50-6.53 (m, 2H, Ar*H*), 6.75-6.78 (d, 2H, J = 8.0Hz, Ar*H*), 7.05-7.47 (m, 10H, Ar*H*). $^{13}$C-NMR ($CDCl_3$, 400 MHz) δ: 173.9, 173.7, 142.4, 141.4, 131.99, 131.90, 129.69, 129.44, 128.10, 127.9, 127.8, 126.5, 126.0, 113.2, 77.3, 77.2, 77.0, 76.7, 74.9, 66.8, 60.0, 56.1, 53.2, 47.9, 42.7, 41.9, 40.4, 40.1, 37.5, 35.8, 35.5, 35.0, 34.6, 33.9, 30.9, 30.5, 29.0, 28.2, 26.6, 26.3, 24.9, 24.2, 23.3, 20.8, 18.5, 13.5, 12.0. ESI-MS: m/z calcd. for $C_{56}H_{77}ClN_2O_5$: 893.67, found: 857.42 $[M]^+$.

**LCA-Tam-PYR:** Yield: 86.7 %. $^{1}$H-NMR ($CDCl_3$, 500 MHz) δ: 0.629 (s, 3H, -C*H*$_3$), 0.856-2.31 (m, 43H), 2.414-2.450 (q, 2H, J = 7.2 Hz, -C*H*$_2$CH$_3$), 2.933-3.068 (d, 3H, -N-C*H*$_3$), 3.613-3.652 (t, 2H, J = 5.5Hz, -N-CH$_2$-C*H*$_2$-O-), 3.93-4.017 (m, 2H, -N-C*H*$_2$-CH$_2$-O- ), 4.82-4.85 (m, 1H, -O-C*H*), 6.258-6.271 (q, 2H, J=5.2, CO-C*H*$_2$-N$^+$-), 6.504-6.525 (d, 2H, J = 8.5Hz, Ar*H*), 6.746-6.785 (m, 2H, Ar*H*), 7.10-7.351 (m, 9H, ArH), 8.05-8.06 (t, 2H, J=13.6 Hz, ArH), 8.452-8.491(t,1H, J=15.6 Hz, ArH), 9.434-9.448 (d, 2H, J = 5.6 Hz, Ar*H*). $^{13}$C-NMR ($CDCl_3$, 400 MHz) δ: 173.7, 165.5, 156.5, 149.6, 145.5, 143.7, 142.4, 142.3, 141.6, 141.4, 138.2, 138.0, 135.6, 131.9, 129.6, 129.4, 128.1, 127.9, 127.8, 127.5, 126.5, 126.0, 113.2, 66.5, 35.1, 61.2, 56.3, 56.0, 49.1, 47.9, 42.7, 41.9, 40.4, 40.0, 37.5, 35.7, 34.9, 34.5, 33.9, 32.0, 30.9, 30.3, 29.7, 29.0, 28.2, 26.9, 26.4, 24.2, 23.2, 20.8, 18.5, 13.5, 12.0. ESI-MS: m/ z calcd. for $C_{56}H_{71}ClN_2O_4$: 871.62, found: 835.38) $[M]^+$.

**LCA-Tam-DMAP:** Yield: 80 %. $^{1}$H-NMR ($CDCl_3$, 500 MHz) δ: 0.627 (s, 3H, -C*H*$_3$), 0.836-2.315 (m, 52H), 2.412-2.466 (q, 2H, J = 7.2 Hz, -C*H*$_2$CH$_3$), 2.933-3.068 (d, 3H, -N-C*H*$_3$), 3.22-3.26 (s, 6H, -N-(CH$_3$)$_2$, 3.613-3.652 (t, 2H, J = 5.5Hz, -N-CH$_2$-C*H*$_2$-O-), 3.93-3.99 (m, 2H, -N-C*H*$_2$-CH$_2$-O- ), 4.76-4.77 (m, 1H, -O-C*H*), 5.43-5.50 (q, 2H, J=5.2, CO-

C*H*$_2$-N$^+$-), 6.53 (d, 2H, J = 7.0Hz, Ar*H*), 6.77 (d, 2H, J = 8.5Hz, Ar*H*), 6.88 (d, 2H, J = 8.0Hz, Ar*H*), 7.12-7.35 (m, 10H, Ar*H*), 8.51 (d, 2H, J = 8.0Hz, Ar*H*). $^{13}$C-NMR ($CDCl_3$, 400 MHz) δ: 173.7, 166.7, 156.5, 144.0, 143.7, 142.4, 141.4, 138.2, 135.6, 131.9, 131.8, 129.6, 128.1, 127.8, 126.5, 126.0, 113.2, 107.5, 66.5, 57.8, 56.3, 55.9, 47.9, 42.7, 41.9, 40.4, 37.5, 35.7, 35.4, 34.9, 34.5, 32.0, 30.9, 30.2, 29.7, 28.2, 26.9, 26.4, 26.2, 24.2, 23.2, 20.8, 18.5, 13.5, 12.0. ESI-MS: m/ z calcd. for $C_{58}H_{76}ClN_3O_4$: 914.69, found: 878.40 $[M]^+$.

**LCA-Tam-DABCO:** Yield 82 %. $^1$H-NMR ($CDCl_3$, 500 MHz) δ: 0.63 (s, 3H, -C*H*$_3$), 0.634-2.42 (m, 52H), 2.412-2.48 (q, 2H, J = 7.2 Hz, -C*H*$_2$CH$_3$), 2.9-3.1 (d, 3H, -N-C*H*$_3$), 3.16-3.27& 3.9-4.1 (m, 12H, 2 x -N-(C*H*$_2$)$_3$), 3.66 (t, 2H, J = 5.5Hz, -N-CH$_2$-C*H*$_2$-O-), 3.95-4.01 (m, 2H, -N-C*H*$_2$-CH$_2$-O-), 4.6-4.9 (m, 3H, , CO-C*H*$_2$-Cl -O-C*H*), 6.53 (d, 2H, J = 7.0Hz, Ar*H*), 6.78 (d, 2H, J = 8.5Hz, Ar*H*), 7.05-7.47 (m, 11H, Ar*H*). $^{13}$C-NMR ($CDCl_3$, 400 MHz) δ: 172.7, 164.2, 141.4, 131.9, 129.6, 129.4, 128.1, 127.8, 126.5, 126.0, 113.2, 66.5, 52.6, 47.9, 45.3, 44.8, 42.7, 41.9, 40.4, 37.5, 35.7, 34.5, 30.9, 29.6, 29.0, 26.9, 26.4, 24.1, 23.2, 20.8, 18.5, 13.5, 12.0. ESI-MS: m/z calcd. for $C_{57}H_{78}ClN_3O_4$: 904.69, found: 868.43) $[M]^+$.

**Laurdan-based hydration studies:** Generalized polarization (GP) studies were performed in a 96-well plate using Molecular Device M5 instrument in end point mode using $\lambda_{ex}$ of 350 nm and $\lambda_{em}$ of 440 and 490 nm respectively. Amphiphiles at a concentration of 30 mol% were incubated with DPPC vesicles containing laurdan as described earlier,[26] and fluoresence was measured at every 6h interval. General polarization (GP) was calculated using equation.[26]

$GP= (I_{440}-I_{490})/ (I_{440}+I_{490})$

**Fluorescence anisotropy studies:** Amphiphiles at a concentration of 30 mol% were incubated with DPPC vesicles containing DPH. Steady state fluorescence anisotropy ($r_{ss}$) of DPH was measured at regular intervals in a 96-well plate with $\lambda_{ex}$ at 350 nm and $\lambda_{em}$ of 452 nm using the equation as described earlier[26]

$r_{ss} = (I_{ll} - G\, I_{\perp}) / (I_{ll} + 2\, G\, I_{\perp})$

**Differential Scanning Calorimetry:** DSC studies have been performed on Nano DSC, TA instruments, USA, on incubation of amphiphiles at a concentration of 30 mol% with DPPC membranes as described earlier.[26]

**Cell culture:** T47D, MCF-7, MDA-MB-231 and MDA-MB-468 cells in DMEM (Sigma, USA) media containing 10% (w/v) fetal bovine serum, penicillin (100 µg/mL), streptomycin (100 U/mL), gentamycin (45 µg/mL) have been maintained at 37 $^{o}$C in a humidified atmosphere with 5% $CO_2$.

**Cytotoxicity assay:** Cell viability for amphiphiles were measured using MTT{3-[4,5-dimethylthiazol-2-yl]-2,5-diphenyltetrazolium bromide} assay. Cells were plated at a density of ~5000 cells per well in 96 wells plates in 200 µL of medium. After 24h, cells were treated with Tam and amphiphiles at a concentration of 1, 5, 10, 20, and 50 µM in fresh medium. After 48h of treatment, 20µL of MTT solution (4 mg/mL) was added to each well and incubated for 3h. Media was aspirated and 200 µL of DMSO:Methanol (1:1) solution was added to dissolve purple formazan crystals whose absorption was measured at 540 nm. Cell viability was then calculated using formula [{A540 (treated cells)-background]/ [A540 (untreated cells-background}] 100.

**Cellular uptake assay:** Cells were plated at a density of ~10,000 cells per well in 24 well plates and were treated at 20µM of Tam-NBD and LCA-DMAP-NBD. After 24h, cells were harvested and washed thrice with PBS followed by centrifugation at 5000 rpm at 4 $^{o}$C for 5 min. Cells were then analysed on a FACS (Becton Dickinson, Mountain View, CA) for uptake studies.

**Cell cycle analysis:** Cells were plated at a density of ~2.0 $\times 10^5$ cells per well in 6 well plates and were treated 10 and 20µM of Tam, LCA-DMAP, and LCA-Tam-DMAP. After 48h, cells were harvested, washed thrice with PBS followed by centrifugation at 5000 rpm at 4 $^{o}$C for 5

min. Cells were fixed in chilled 70% ethanol and stained with 50µg/mL propidium iodide at room temperature for 10 min. Cells were then counted on a FACS (Becton Dickinson, Mountain View, CA), and percentages of cells in sub $G_0$, $G_0/G_1$, $G_1$, S and $G_2$/M phases of the cell cycle were determined using Mod Fit LT software (Verity Software House, Topsham, ME).

**ROS measurements:** Intracellular ROS levels were measured using dichlorodihydrofluoresceindiacetate (DCFDA, Sigma USA) according to earlier protocols.[18] Briefly, DCFDA labeled cells were treated with Tam, LCA-DMAP and LCA-Tam-DMAP at 10 and 20 µM concentration. Fluorescence emission was recorded using 96 well plate reader (Spectramax pro 5) using excitation and emission wavelengths of 485 and 535 nm up to 1 h at the interval of 15 min. The experiments were repeated at least three times.

**Mitochondrial transmembrane potential ($\Delta\psi_m$) measurements:** Change in mitochondria transmembrane potential ($\Delta\psi_m$) was assessed by determining the accumulation of 3,3′-dihexyloxacarbocyanine iodide [$DiOC_6$] (Sigma, USA) in mitochondrial matrix.[27] $DiOC_6$ is a membrane permeable dye which stains mitochondria. Amount of dye retained in the cell will correspond to its viability. Cells were plated at density of ~$2.0 \times 10^5$ cells per well in 6 well plates. After 24h, media was removed and cells were treated with 10 and 20µM of Tam, LCA-DMAP, and LCA-Tam-DMAP in fresh media for 48h at 37 $^oC$ incubator. Before harvesting, cells were incubated with 50 nM $DiOC_6$ at 37 °C for 30 min. Cell were harvested and analysed on a BD FACS (Becton Dickinson). Data were gated to exclude debris, and number of cells losing mitochondiral fluorescence were plotted.

**Western studies:** Expression levels of apoptotic proteins were studied using immunoblotting according to earlier protocols.[18] Briefly, Tam, LCA-DMAP, and LCA-Tam-DMAP treated cells for 48 h were trypsinzed; pellets were collected, and washed with ice-cold PBS. Cells were lysed in RIPA buffer using protease inhibitor cocktail for 45 min at 4 °C. Cell lysate was

centrifuged at 13,000 rpm for 15 min at 4 °C and supernatant was collected. Equal amount of proteins were loaded on 10% SDS-polyacrylamide gel and transferred to nitrocellulose membrane. Membranes were blocked with 5% of skimmed milk in PBST and probed with primary antibodies (Cell Signaling Technologies, NEB, Frankfurt, Germany) overnight at 4 $^{o}$C, followed by washing in PBS (3x) containing 0.5% Tween-20. Blots were re-probed with β-actin antibody as an internal control. Secondary anti Rabbit HRP conjugated antibody was used for all antibodies except for β-actin where anti mouse secondary HRP conjugated antibody was used. Results were analyzed and documented using GE image quant and documentation software (Image Quant LAS 4000).

**Acknowledgments:** We thank Regional Centre for Biotechnology for intramural funding and Department of Biotechnology (DBT) for funding this project. SB and SG thank DBT, and KY and VS thank RCB for research fellowship. AB thanks DST for Ramanujan fellowship. We thank Dr. Nirpendra Singh for helping in mass spectral studies, and Mr. Vijay Kumar Jha for helping in calorimetry experiments.

**Author contributions:** AB conceived the idea and designed the experiments. PB synthesized all the compounds. PB and MS performed the biophysical experiments. KY and SB performed the cell biology and biochemical experiments. SG performed the HPLC studies. SK and VS synthesized Tam-NBD and LCA-DMAP-NBD amphiphiles. AB, KY, SB, and PB analyzed the results and written the manuscript.

†Electronic Supplementary Information (ESI) available: [MTT graphs, Synthesis of Tam-NBD and LCA-DMAP-NBD, $^{1}$H-NMR, HRMS, and HPLC spectra]. See DOI: 10.1039/b000000x/

1. H. Rosen, and T. Abribat, *Nat. Rev. Drug Discov.* 2005, **4**, 381.
2. T. M. Allen, and P. R. Cullis, *Science* 2004, **303**, 1818.
3. C. Peetla, A. Stine, and V. Labhasetwar, *Mol. Pharm.* 2009, **6**, 1264.
4. B. H. Lerner, *Nat. Rev. Cancer.* 2002, **2**, 230.

5. E. C. Dreaden, S. C. Mwakwari, Q. H. Sodji, A. K. Oyelere, and M. A. EI-Sayed, *Bioconjug. Chem.* 2009, **20**, 2247.
6. J. B. Tange, S. Kakumanu, D. Ortiz, T. Shea, and T. J. Nicolosi, *Mol. Pharm.* 2008, **5**, 280.
7. A. K. Jain, N. K. Swarnakar, C. Godugu, R. P Singh, and S. Jain, *Biomaterials.* 2011, **32**, 503.
8. S. K. Mishra, P. Kondaiah, S. Bhattacharya, and C. N. Rao, *Small*. 2012, **8**, 131.
9. G. Zhang, I. Kimijima, M. Onda, M. Kanno, H. Sato, T. Watanabe, A. Tsuchiya, R. Abe, and S. Takenoshita, *Clin. Cancer Res.* 1999, **5**, 2971.
10. M. Engelk, P. Bojarski, R. Bloss, and H. Diehl, *Biophys. Chem.* 2001, **90**, 157.
11. J. B. Custodio, L. M. Almeida, and V. M. Madeira, *Biochim. Biophys. Acta* 1993, **1150**, 123.
12. V. C. Jordan, *Eur. J. Cancer* 2008, **44**, 30.
13. (a) Y. Zheng, H. Fu, M. Zhang, M. Shen M. Zhu, and X. Shi, *Med. Chem. Commun.* 2014, **5**, 879. (b) C. Hess, D. Venetz, and D. Neri, *Med. Chem. Commun.* 2014, **5**, 408. (c) H. Dong, C. Dong, W. Xia, Y. Li, and T. Ren, *Med. Chem. Commun.* 2014, **5**, 147. (d) M. Singh, A. Singh, S. Kundu, S. Bansal, and A. Bajaj, *Biochim. Biophys. Acta* 2013, **1828**,1926.
14. (a) H. K Agarwal, B. S. Chhikara, S. Bhavaraju, D. Mandal, G. F. Doncel, and K. Parang, *Mol. Pharm.* 2013, **10**, 467. (b) S. Patil, S. Gawali, S. Patil, and S. Basu, *J. Mater Chem. B* 2013, **1**, 5742. (b) S. Patil, S. Patil, S. Gawali, S. Shende, S. Jadhav, and S. Basu, *RSC Adv.* 2013, **3**, 19760. (c) I. M. Herzog, M. Feldman, A. Eldar-Boock, R. Santchi-Fainaro, and M. Fridman, *Med. Chem. Commun.* 2013, **4**, 120. (d) M. Y. Fosso, Y. Li, S. Garneau-Tsodikova, *Med. Chem. Commun.* 2014, **5**, 1075. (e) C. –W. T. Chang, and J. Y. Takemoto, *Med. Chem. Commun.* 2014, **5**, 1048. (f) I. M. Herzog, and M. Fridman, *Med. Chem. Commun.* 2014, **5**, 1014.
15. a) G. Sudhakar, S. R. Bathula, and R. Banerjee, *Eur. J. Med. Chem.* 2014, **86**, 653; b) S. Sau, and R. Banerjee, *Eur. J. Med. Chem.* 2014, **83**, 433; c) K. Pal, S. Pore, S. Sinha, R. Janardhanan, D. Mukhopadhyay, and R. Banerjee, *J. Med. Chem.* 2011, **54**, 2378.

16. (a) S. Mukhopadhyay, and U. Maitra, *Curr. Sci.* 2004, **87**, 1666. (b) A. Gioiello, F. Venturonu, S. Tamimi, C. Custodi, R. Pellicciari, and A. Macchiarulo, *Med. Chem. Commun.* 2014, **5**, 750.
17. O. Briz, M. A. Serrano, N. Rebollo, B. Hagenbuch, P. J Meier, H. Koepsell, and J. J. G Marin, *Mol. Pharmacol.* 2009, **61**, 853.
18. V. Sreekanth, S. Bansal, R. K. Motiani, S. Kundu, S. Muppu, T.Majumdar, K.Panjamurthy, S. Sengupta, and A. Bajaj, *Bioconjug. Chem.* 2013, **24**, 1468.
19. (a) A. Bajaj, S. K. Mishra, P. Kondaiah, and S. Bhattacharya, *Biochim. Biophys. Acta* 2008, **1778**, 1222. (b) S. Bansal, M. Singh, S. Kidwai, P. Bhargava, A. Singh, V. Sreekanth, R. Singh, and A. Bajaj *MedChemCommun* 2014, **5**, 1761. c) M. Singh, S. Bansal, S. Kundu, P. Bhargava, A. Singh, R. K. Motiani, R. Shyam, V. Sreekanth, S. Sengupta, and A. Bajaj, *Med. Chem. Commun.* 2015, DOI: 10.1039/C4MD00223G.
20. (a) T. Parasassi, E. K. Krasnowska, L. Bagatolli, and E. Gratton, *J. Fluoresc*. 1998, **8**, 365. (b) V. Sreekanth, and A. Bajaj. *J. Phys. Chem. B.* 2013,**117**, 2123.
21. V. Sreekanth, and A. Bajaj, *J. Phys. Chem. B.* 2013, **117**, 12135.
22. S. Bhattacharya, and A. Bajaj, *Langmuir* 2007,**23**, 8988.
23. J. Sonnemann, C. Marx, S. Becker, S. Wittig, C. D. Palani, O. H. Kramer, and J. F. Beck *Br.J. Cancer* 2014, **110**, 656.
24. A. Kallio, A. Zheng, J. Dahllund, K. M. Heiskanen, and P. Harkonen, *Apoptosis*. 2005, **10**, 1395.
25. U. J Reiner, *Breast Cancer Res. Treat.* 2009, **117**, 219.
26. P. Bhargava, M. Singh, V. Sreekanth, and A. Bajaj. *J. Phys. Chem. B* 2014, **118**, 9341.
27. U. Ozgen, S. Savaşan, S. Buck, and Y. Ravindranath, *Cytometry* 2000, **42**, 74.